EPSC Abstracts
Vol. 13, EPSC-DPS2019-352-3, 2019
EPSC-DPS Joint Meeting 2019
© Author(s) 2019. CC Attribution 4.0 license.

EPSC
EPSC-DPS Joint Meeting 2019
15–20 September 2019 | Geneva, Switzerland

3-µm Reflectance Spectroscopy of Outer Main Belt Asteroids: Context and Implications

D. Takir[1], W. Neumann[2], S.N. Raymond[3], J.P. Emery[4]. [1] JETS/ARES, NASA JSC, Houston, TX (driss.takir@nasa.gov), [2]German Aerospace Center, Institute of Planetary Research, Berlin, Germany, [3]Laboratoire d'Astrophysique de Bordeaux, Bordeaux, France, [4]University of Tennessee, Knoxville, TN

Abstract

We present 3-µm spectra of 50 new Outer Main Belt asteroids, which were observed using the NASA Infrared Telescope Facility (IRTF). The new and previous asteroid observations are placed in the context of the current thermal and dynamical theories.

1. Introduction

Most primitive asteroids are concentrated in the Outer Main Belt (OMB), spanning the 2.5 < a < 4.0 AU region. These carbon-rich and low-albedo are important because they provide additional information related to the abundance and distribution of minerals and chemical compounds in the early solar system. Such information will then allow more constraints on the current dynamical and thermal theories of the formation and evolution of the early solar system. OMB asteroids are thought to be originally composed of mixtures of anhydrous materials and water ice. The melted ice, by the released heat from decay of short-lived radionuclides, reacted with anhydrous materials (e.g., olivine, pyroxene) to form hydrated minerals [1]. The snow-line falls within the heliocentric range in which our studied OMB asteroids are concentrated. Its location may have been drifted inwards due to the disk evolution and change of the temperature structure [2] or during the nebular evolution (e.g., [3]). Recent dynamical models (e.g., [4,5]) suggested that a substantial fraction of OMB asteroids originated between or beyond the giant planets (a > 5 AU), where water ice would have been stable, and then implanted in the OMB space as a consequence of the giant planets' growth. Here, we present new 3-µm spectral analysis of 50 OMB asteroids, which were observed using the NASA Infrared Telescope Facility (IRTF). The new asteroid observations are placed in the context of the current thermal and dynamical theories.

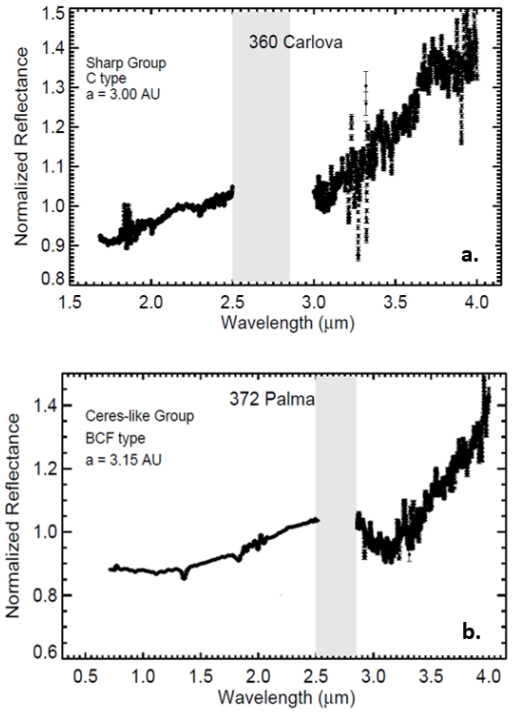

Figure 1. (a) Example of an asteroid, 360 Carlova, with sharp 3-µm feature. (b) Example of an asteroid, 372 Palma, with asteroid Europa-like feature.

2. Results

We measured spectra of OMB asteroids with the long-wavelength cross-dispersed (LXD: 1.9- 4.2 µm) mode of the SpeX spectrograph/imager at IRTF [6]. We obtained LXD data of asteroids over the course of multiple semesters between 2015 and 2018. We used the IDL (Interactive Data Language)-based spectral reduction tool Spextool (v4.0) [7] to reduce the data. We removed the thermal excess in

asteroids' spectra using the methodology described in [8] and references therein. Most of the newly-observed OMB asteroids exhibit a characteristically sharp 3-μm feature attributed to OH-stretching in hydrated minerals (e.g., serpentine) (e.g., Figure 1a). The majority of asteroids in this group are concentrated in the 2.5 < a < 3.3 AU region. We also identified new additional asteroids with Europa-like feature (e.g., Figure 1b), located in the ~3.0 < a < 3.2 AU region. This 3-μm feature is possibly due to phyllosilicates that allow interlayer H_2O (along with OH).

3. Thermal modeling and evolution of OMB asteroids

Calculations of thermal evolution of rocky and icy planetesimals were performed using 1D finite differences thermal evolution models [9,10]. Such models consider heating of small bodies after accretion and the evolution of their temperature and structure. In particular, porosity and compaction due to hot pressing of an initially unconsolidated interior is included. For rocky bodies, an ordinary chondritic composition with a material that is dominated by olivine was assumed. For icy bodies, an ice-rich composition with 25 vol% H_2O and a rock fraction that contains 85 vol% phyllosilicates and 15 vol% olivine upon aqueous alteration was assumed. An initial porosity of 40% is reduced following the change of the strain rate that is calculated as a volume fraction weighted arithmetic mean of strain rates of components. Material properties (thermal conductivity, density, heat capacity, etc.) correspond to the composition assumed and are adjusted with temperature and porosity. Melting of metal and silicates (rocky bodies) or water ice (icy bodies) as well as metalsilicate and water-rock separation are included. Both short- and long-lived radionuclides are considered as heat sources. The initial temperature is either 290 K (rocky bodies) or 170 K (icy bodies). Figure 2 shows the maximum temperature calculated for both types of bodies (3a: rocky, 2b: icy) as a function of radius and accretion time. A variety of internal structures is obtained in both cases, ranging from primordial (2a: no melting of metal and silicates; 2b: no melting of water ice) over partially differentiated (2a: melting of metal and/or silicates, formation of an iron core and silicate mantle below an undifferentiated layer; 2b: melting of water ice, formation of a rocky core and water ocean below an undifferentiated layer) to completely differentiated ones (2a: iron core, silicate mantle with a magma ocean, Vesta-like case; 2b: rocky core, water mantle, Enceladus-like case). The heating and differentiation of planetesimals is determined by the availability of 26Al, i.e., by the accretion time t0 relative to the formation of the calcium-aluminum-rich inclusions (CAIs), such that maximum temperatures and structures vary strongly for t0 < 4 Myr rel. to CAIs. However, for a later accretion only the size of the body determines its maximum temperature and structure due to the nearly constant heating by long-lived radionuclides.

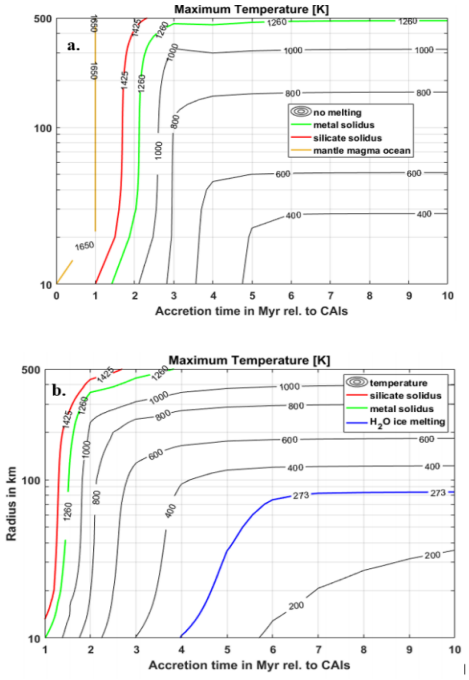

Figure 2: Maximum temperature for rocky (a) and icy (b) planetesimals as a function of the accretion time rel. to CAIs and of the radius.

[1] Grimm, R.E., McSween, H.Y. (1993). Science 259, 653–655.
[2] Cyr K.E. et al. (1998) Icarus 135, 537-548.
[3] Dodson-Robinson S.E. et al. (2009) Icarus 200, 672–693.
[4] Walsh K.J. et al. (2013) Nature 475, 206-209.
[5] Raymond S.N. and Izidoro A. (20170 Icarus 297, 134-148.
[6] Rayner J.T. (2003) ASP 155, 362- 382.
[7] Cushing M.C. (2004) ASP, 166, 362-376.
[8] Takir D. and Emery J.P. (2012) Icarus, 219, 641-654.
[9] Neumann W. et al. (2018) Icarus, 311, 146-169.
[10] Neumann W. et al. (2017) ACM 2017, Parallel1.a.4.